

# **Novel functionalized carbon nanotube supercapacitor materials**

*Contribution to the supercapacitor TIF*

Trisha Huber

**Defence Research and Development Canada**

Scientific Report

DRDC-RDDC-2014-R63

August 2014



# **Novel functionalized carbon nanotube supercapacitor materials**

*Contribution to the supercapacitor TIF*

Trisha Huber

**Defence Research and Development Canada**

Scientific Report

DRDC-RDDC-2014-R63

August 2014

- © Her Majesty the Queen in Right of Canada, as represented by the Minister of National Defence, 2014
- © Sa Majesté la Reine (en droit du Canada), telle que représentée par le ministre de la Défense nationale, 2014

## **Abstract**

---

Numerous functionalized carbon nanotube materials, utilizing a variety of means, were prepared and characterized with respect to their charge storage capability. These materials exploit the high surface area and dc conductivity of carbon nanotubes, while introducing a pseudocapacitive charge storage mechanism through judicious functionalization. The effect on the capacitance of functionalizing with conjugated polymers, conducting polymers, and ruthenium oxide, are reported here. Through functionalization at the nanoscale level, improvements to capacitance were realized.

## **Significance to defence and security**

---

Lightweight energy storage and high power density energy storage devices are of interest to the military, particularly for the dismounted soldier, silent watch operations, and high power devices. The intent of this project was to develop lightweight materials that exhibit higher power density than batteries, and higher energy density than commercially available capacitors. The prepared active materials exhibited relatively high energy density, however, measuring their power density is more complex, and requires additional effort.

## Résumé

---

On a préparé et caractérisé, en utilisant diverses méthodes, de nombreux matériaux fonctionnalisés pour nanotubes de carbone, selon leur capacité d'accumulation de charge. Les matériaux de ce type présentent des avantages associés à la grande surface efficace et à la conductivité élevée (en c.c.) des nanotubes de carbone, ainsi qu'un nouveau mécanisme d'accumulation de charge pseudocapacitive, lequel est obtenu en réalisant une fonctionnalisation judicieuse. Le présent rapport traite, entre autres, des effets de la fonctionnalisation du matériau sur sa capacité, notamment dans le cas de sa fonctionnalisation avec des polymères conjugués, des polymères conducteurs et de l'oxyde de ruthénium. En effectuant une fonctionnalisation à l'échelle nanométrique, il a été possible d'accroître la capacité des matériaux à l'étude.

## Importance pour la défense et la sécurité

---

Les dispositifs d'accumulation d'énergie légers et ceux à densité de puissance élevée sont d'un grand intérêt pour les intervenants de divers domaines militaires, particulièrement ceux qui réalisent des travaux de recherche sur les dispositifs utilisés par les soldats débarqués et lors d'opérations de veille silencieuse, et sur les dispositifs à forte puissance. Les travaux du présent projet ont pour objectif de mettre au point des matériaux légers qui présentent une densité de puissance supérieure à celle des piles et une énergie volumique supérieure à celle des condensateurs commerciaux. Les matériaux actifs préparés présentent une énergie volumique relativement élevée, mais la mesure de leur densité de puissance est plus complexe et des efforts additionnels devront être consacrés à cette tâche.

# Table of contents

---

Abstract .....	i
Significance to defence and security .....	i
Résumé .....	ii
Importance pour la défense et la sécurité .....	ii
Table of contents .....	iii
List of figures .....	iv
List of tables .....	vi
Acknowledgements .....	vii
1 Introduction .....	1
2 Polymer functionalization of carbon nanotubes .....	5
2.1 Preparation of films from poly(styrene sulfonate) – SWNT composites .....	5
2.2 Preparation of SWNTs functionalized with conjugated polymers .....	6
2.3 Supramolecular functionalization of SWNTs with conjugated polymers .....	6
2.4 Supramolecular functionalization of SWNTs with conjugated polyelectrolytes .....	8
2.4.1 Patterning of conjugated polyelectrolyte-functionalized SWNTs .....	8
2.4.2 Electrophoretic deposition .....	10
2.5 Supramolecular functionalization of SWNTs with sulfonated polyaniline .....	12
2.6 Results .....	12
2.7 Conclusions .....	13
2.8 Most significant results .....	14
3 Conducting polymer – carbon nanotube composites .....	15
3.1 Purity and functionalization of CNTs .....	15
3.2 Active material screening protocol .....	16
3.3 The effect of dopant on capacitance .....	17
3.4 Conclusions .....	23
3.5 Most significant results .....	24
4 Ruthenium oxide – carbon nanotube composites .....	25
4.1 Synthesis and characterization .....	25
4.2 Conclusions .....	31
4.3 Most significant results .....	31
5 Conclusions and future work .....	33
References .....	35
List of symbols/abbreviations/acronyms/initialisms .....	37

## List of figures

---

Figure 1	Ragone plot comparing the power density and energy density of various energy storage devices.....	2
Figure 2	Diagram of a conventional capacitor. ....	2
Figure 3	Maximizing the surface area with a high porosity material (a). Electric double layer yields a charge separation in the order of several nanometers (b).....	3
Figure 4	Schematic representation of nanotube thin film formation by filtration of a dilute nanotube solution through a porous membrane, with an AFM image of the resulting film at right. ....	5
Figure 5	Suzuki polycondensation for the preparation of carbon nanotubes functionalized with conjugated polymers.....	6
Figure 6	Supramolecular assembly of conjugated polymers onto the surface of SWNTs. ....	7
Figure 7	Chemical structures of the two CPEs used for nanotube functionalization. ....	8
Figure 8	(A) Pattern of squares, imaged by optical profilometry, formed by immersing a pre-patterned glass slide with 90- $\mu\text{m}$ squares of cross-linked PVMP into an aqueous solution of a-PP-SWNTs. (B) Cross-sectional height vs. distance plot of the sample shown in (A), where the black line indicates the location of the cross section. ....	9
Figure 9	SEM images of patterned SWNTs on a glass substrate. A and B represent images of the substrate at two different magnifications, while C and D represent further magnified images of the areas marked with a white circle and square in image B, respectively. ....	10
Figure 10	Schematic representation of electrophoretic deposition of appropriately functionalized carbon nanotubes onto an electrode surface. ....	11
Figure 11	Electrophoretically deposited films of CPE-functionalized SWNTs. (A) Image of a relatively thin film of approximately 200 nm thickness; (B) Thicker film of approximately 2 micron thickness; (C) Close-up of the film in (B) showing the presence of nanotubes within the deposit. ....	11
Figure 12	Specific capacitance of SPA-SWNT (a) and SPA-MWNT (b).....	12
Figure 13	High resolution TEM (HRTEM) of a specimen reveals individual SWCNTs wrapped with polymer (see arrow). ....	13
Figure 14	Cyclic voltammetry data demonstrate the reproducibility of the electrode preparation (scan rate 10 mV/s).....	16
Figure 15	DC conductivity for polyaniline doped with acids (dopants) of varying size and shape. ....	17
Figure 16	A repeat unit for doped polyaniline, in which the dopant anion is represented as A-.....	18
Figure 17	Dopant structure and transmission electron microscope (TEM) images of MWCNTs coated with a) PAni-PTSA, b) PAni-DBSA, and c) PAni-2NSA. ....	19
Figure 18	Cyclic voltammogram showing capacitance as a function of potential for	20



	PA <sub>ni</sub> /PTSA-MWCNT, PA <sub>ni</sub> /DBSA-MWCNT, and PA <sub>ni</sub> /2-NSA-MWCNT. All materials contain ~42% MWCNT. The capacitance has been normalized to exclude dopant mass.....	
Figure 19	Plot of capacitance versus polymer content for PA <sub>ni</sub> /2-NSA-MWCNT composites using both thin (10 nm diameter) and thick (30 – 50 nm diameter) MWCNTs. ....	21
Figure 21	Plot of capacitance versus polymer content for PA <sub>ni</sub> /2-NSA-MWCNT composites prepared by the standard protocol, as well as using an iterative approach, and dispersing the MWCNTs for a longer period of time. ....	23
Figure 22	TEM of a 25.1% Ru oxide/p-MWCNT composite. ....	26
Figure 23	TEM of a 15.6% Ru oxide/a-MWCNT composite.....	27
Figure 24	Cyclic voltammograms at 20 mV s <sup>-1</sup> of p-MWCNT and a-MWCNT. ....	28
Figure 25	Cyclic voltammograms at 20 mV s <sup>-1</sup> for 25.1 % Ru oxide/p-MWCNT (solid), blank p-MWCNT (dotted) and the calculated specific capacitance of the Ru oxide component of the composite (dashed).....	29
Figure 26	Cyclic voltammograms at 20 mV s <sup>-1</sup> for 15.6 % Ru oxide/a-MWCNT (solid), blank a-MWCNT (dotted) and the calculated specific capacitance of the Ru oxide component of the composite (dashed).....	29
Figure 27	Cyclic voltammogram at 50 mV s <sup>-1</sup> of a full cell of 25.1% Ru oxide/p-MWCNT. Each electrode was comprised of approximately 5 mg of active material. ....	30
Figure 28	Charging (○) and discharging (●) times between 0V and 1V at a rate of 100 mA/cm <sup>2</sup> . Note the initial increase in time and the stability up to 20 000 cycles.....	31

## List of tables

---

Table 1	Conductivity data for nanotube thin films.....	7
Table 2	Capacitance values for the same electrode made with PAni-2NSA/MWCNT, based on different measurement methods.....	16

## Acknowledgements

---

The author would like to acknowledge the contribution of the following people: Alex Adronov, Peter Pickup, Catherine Chow, Felix Wong, Mike Kopac, Scott McClelland, Dave Edwards, and Bruce Kaye.

This page intentionally left blank.

# 1 Introduction

---

The Canadian Forces require a wide range of energy storage to supply power for a variety of military applications. These power requirements span many orders of magnitude from milliwatts (mW) to megawatts (MW). Examples of devices/platforms that require power include micro electro mechanical devices (MEMs), portable battery packs, unmanned aerial vehicles (UAVs), light armoured vehicles (LAVs), kinetic energy/directed energy (KE/DE) weapons, radiofrequency (RF) munitions, remote communications and surveillance, and portable electronics [1].

Pulse power technology was identified as one of three areas in which significant R&D opportunities exist. Presently there is a deficiency of power sources capable of supplying adequate pulse power for many applications including portable electronics, future weaponry, and communications. High pulse power applications require that energy is supplied at a very high rate. Conventional high energy density sources, such as batteries can store a lot of energy (high energy density), however the rate at which this energy can be accessed is relatively slow (low power density). Conversely, conventional capacitors can supply stored energy at very high rates (high power density), although the amount of energy that can be stored is relatively low (low energy density). Thus the capacitor can supply a transient power pulse, but the pulse is very short owing to the low energy density.

The performance of various devices are often compared in a Ragone plot (see Figure 1), in which power density and energy density are presented as a log-log plot. As illustrated, supercapacitors offer performance intermediate between batteries and capacitors in that they exhibit higher energy density than capacitors and higher power density than batteries. Hybrid energy devices, in which a supercapacitor is coupled to a high energy density device (battery or fuel cell), would satisfy high pulse power as well as high energy density requirements.

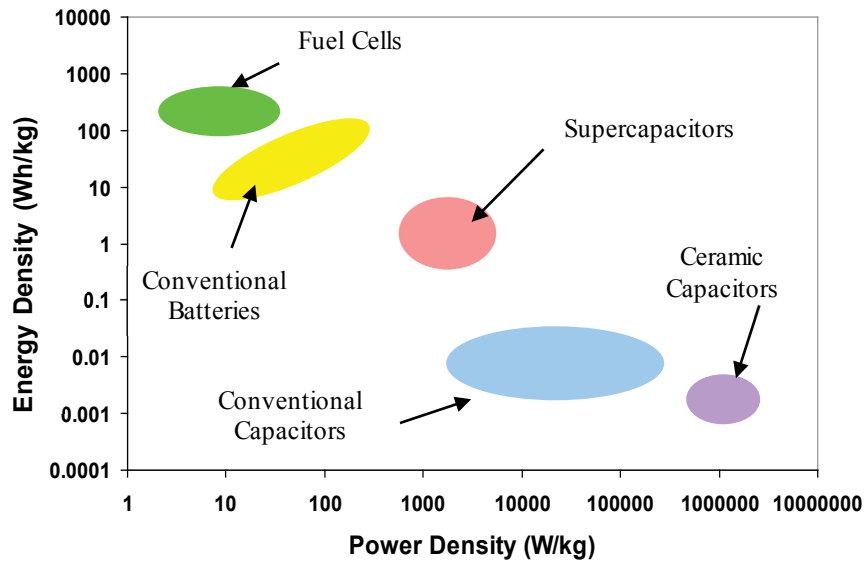


**Figure 1:** Ragone plot comparing the power density and energy density of various energy storage devices.

The increase in capacitance offered by supercapacitors over conventional or parallel plate, capacitors may be easily understood by first considering the charge storage mechanism utilized by conventional capacitors. A parallel plate capacitor consists of two plates (or electrodes), which are connected to a voltage supply and separated by a dielectric material of thickness,  $d$  (see Figure 2). The energy that can be stored in the capacitor is dependent on the capacitance,  $C$ , and the square of the voltage difference between the plates:

$$E = \frac{1}{2} CV^2 \quad (1)$$

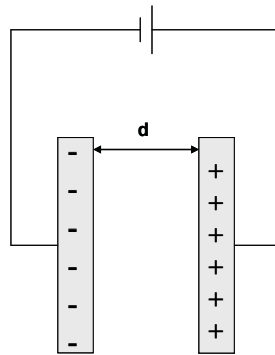


**Figure 2:** Diagram of a conventional capacitor.

The capacitance is dependent on the surface area of the plates, the dielectric constant of the dielectric material, and inversely proportional to the distance between the plates (thickness of the dielectric material),  $d$ :

$$C = \epsilon \frac{A}{d} \quad (2)$$

Supercapacitors, also known as electrochemical capacitors, exhibit capacitances that are several (up to 8) orders of magnitude higher than conventional capacitors, as a result of increasing the surface area ( $A$ ) and decreasing the charge separation ( $d$ ). The use of highly porous or fibrous active materials increases the surface area considerably (Figure 3a). The reduction in charge separation distance is achieved through the use of an electrolyte which, upon charging of the cell, forms a layer of ions close to the surface of the active material (Figure 3b). This layer forms a virtual plate that is separated from the active material surface by solvent molecules, which are effectively the dielectric material. Thus, each electrode of a supercapacitor is in essence a conventional capacitor, and in full cell, the two electrodes are separated by a membrane, which allows ionic, but not electronic, flow.

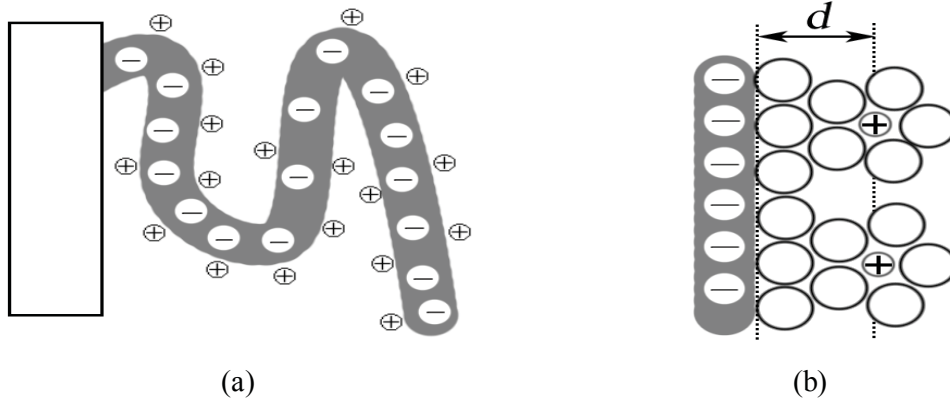


**Figure 3:** Maximizing the surface area with a high porosity material (a). Electric double layer yields a charge separation in the order of several nanometers (b).

Thus, the entire supercapacitor cell is effectively two capacitors (having capacitance  $C_1$  and  $C_2$ ), connected in series; the total capacitance ( $C_{\text{total}}$ ) of which is determined as follows:

$$\frac{1}{C_{\text{total}}} = \frac{1}{C_1} + \frac{1}{C_2} \quad (3)$$

In addition to electrochemical double layer capacitance (EDLC) illustrated above, materials that exhibit redox activity may utilize an additional charge storage mechanism that is pseudo-Faradaic in nature in which charge is stored through reduction or oxidation of the material itself. Materials that exhibit this type of capacitance, called pseudo-capacitance, include transition metal oxides which may be oxidized and reduced, and conducting polymers, in which the charge storage mechanism involves the reversible reduction and oxidation of the backbone chain.

Thus, desirable materials properties include high surface area, optimal porosity (to facilitate fast charging and discharging), redox activity (to enhance charge storage capability), and mechanical robustness (to ensure reasonable time for operability).

To address the requirement for high power energy devices, the Supercapacitor TIF is geared toward developing pulse power technology. In this report, we present the Dockyard Lab Pacific contributions to the Supercapacitor TIF (12sz07). This contribution encompasses part of the effort under the TIF, and is comprised of carbon nanotube-based research. Work was performed in the labs of Alex Adronov at McMaster University and Peter Pickup at Memorial University, under contract; in-house work was also performed at the DRDC Atlantic, Dockyard Lab Pacific.

This report is laid out as follows: Section 2 provides highlights of research performed at McMaster University, Section 3 provides highlights of research performed at the Dockyard Lab Pacific, and Section 4 highlights collaborative work performed at Dockyard Lab Pacific and Memorial University.



## 2 Polymer functionalization of carbon nanotubes

---

This section of the report covers research performed by Alex Adronov's group at McMaster University. The goal of this component of the project was to prepare polymer functionalized single-walled carbon nanotubes (SWNTs) that exhibit promise as supercapacitor electrode materials. SWNTs, which exist in bundles of ropes, exhibit very large surface area ( $\sim 1300 \text{ m}^2/\text{g}$ ) [2]. Effective exploitation of this surface area requires that the SWNTs be deaggregated such that individual tubes have been exfoliated and are stable. The Adronov group have enjoyed success at deaggregating SWNTs resulting from complexation of individual nanotubes by conjugated polymers. HRTEM images indicate that sonication of SWNTs in the presence of complexing polymers results in effective deaggregation; plasma etched specimens show that individual tubes have been complexed by the polymer.

### 2.1 Preparation of films from poly(styrene sulfonate)–SWNT composites

Initial studies carried out at McMaster University were based on poly(styrene sulfonate) (PSS) functionalized SWNTs, using previously reported methodology [3]. Thin films of the water soluble material were formed using a vacuum filtration method outlined in Figure 4. This method involves vacuum filtration of a dilute dispersion of the material through a membrane. The film is collected on the surface of the membrane. This filtration protocol permits the formation of a variety of film thicknesses.

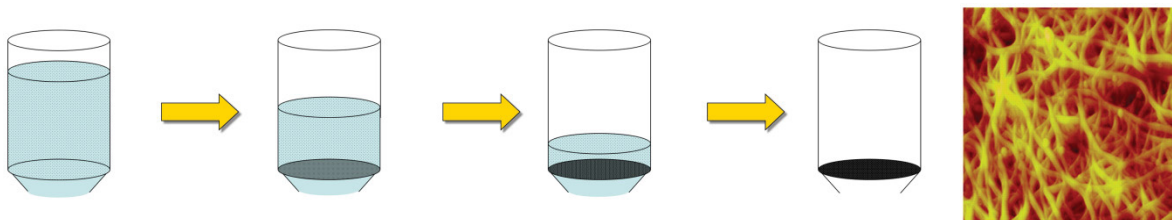


**Figure 4:** Schematic representation of nanotube thin film formation by filtration of a dilute nanotube solution through a porous membrane, with an AFM image of the resulting film at right.

The PSS functionalized SWNTs were found to exhibit greater robustness (highly flexible) compared to films formed with pristine SWNTs. The electrical conductivity of the composites was substantially lower than that of the pristine tubes; this may be attributed to the tubes being well-coated by the insulating polymer, thereby inter-tube charge transfer was impeded.

## 2.2 Preparation of SWNTs functionalized with conjugated polymers

Conjugated polymers were covalently linked to the surface of the nanotubes, using a Suzuki coupling protocol developed in the Adronov lab [4]. The resulting composites were much more easily processible owing to the solubility of the polymers. The linking moiety is conjugated (see Figure 5), and it was anticipated that charge transfer could occur between the nanotubes and the conjugated polymer via the conjugated linker. Although films fabricated as outlined above were highly flexible, they suffered similar electrical conductivity issues as the PSS-functionalized tubes. This may be attributed to insufficient conductivity of the conjugated polymers, poor electronic communication between the polymer and nanotubes, or reduced conductivity of the nanotubes as a result of the covalent functionalization. Covalent functionalization effectively introduces a defect in the extended  $\pi$  system of the nanotubes, thereby reducing the electrical conductivity.

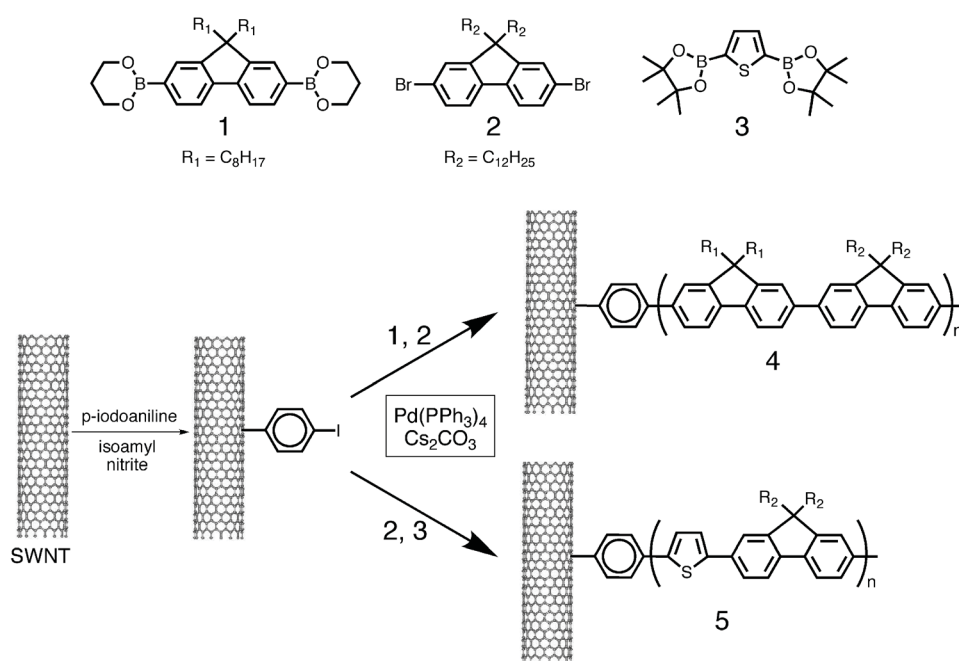


**Figure 5:** Suzuki polycondensation for the preparation of carbon nanotubes functionalized with conjugated polymers.

## 2.3 Supramolecular functionalization of SWNTs with conjugated polymers

In order to address whether the low conductivity is a result of the covalent functionality on the nanotube surface, noncovalent (supramolecular) functionalization of SWNTs with conjugated polymers was carried out. Composites involving four different conjugated polymers were prepared and it was found that the polymers were irreversibly bound to the surface of the NTs. The polymers were derivatives of polyfluorene (6), poly(fluorene-co-thiophene) (7),

polythiophene (8), and a poly(porphyrin-diacetylene) (9) (see Figure 6 for structures). Films prepared from these composites were highly flexible and exhibited improved conductivity over previously prepared composites (see Table 1), in which the polymers were covalently bonded to the nanotubes via a conjugated linker.

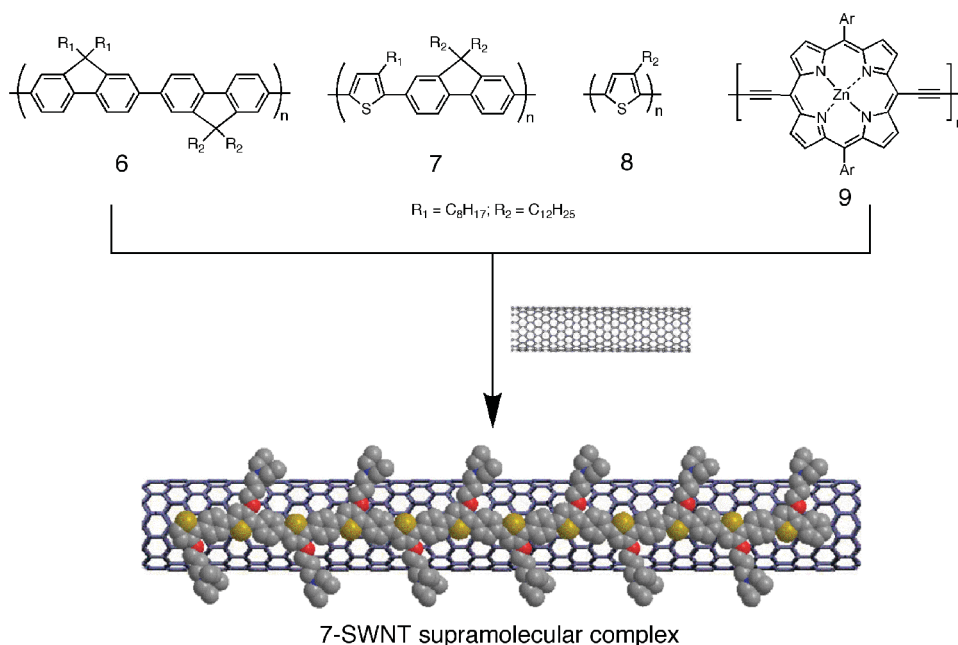


**Figure 6:** Supramolecular assembly of conjugated polymers onto the surface of SWNTs.

**Table 1:** Conductivity data for nanotube thin films.

Sample	Sheet Resistance ( $\Omega$ ) <sup>*</sup>	Thickness (mm) <sup>†</sup>	Conductivity (S/cm)
SWNT	0.70	0.09	160
4-SWNT	$1.1 \times 10^6$		
6-SWNT	1.4		
7-SWNT	3.1	0.05	64
8-SWNT	3.9		
9-SWNT	40	0.04	6.2

<sup>\*</sup> technically the units are ohms per square.

<sup>†</sup> ( $\pm 0.02$  mm).

As with the covalently bonded polymers, SWNT composites of polyfluorene (PF-SWNT) and poly(fluorene-co-thiophene) (PFT-SWNT) were found to exhibit enhanced solution processibility; the resulting SWNT solubility imparted by the polymers was determined to be 322 mg/L and 360 mg/L for the PF-SWNT and PFT-SWNT, respectively. The degree of the electronic interaction between the polymers and the SWNTs was investigated by UV-Vis and fluorescence spectroscopy; results indicate that strong interaction between the components exists.

Capacitance measurements of these polymers indicate relatively low capacitance ( $\sim 10$  F/g), and the film resistances were relatively high.

## 2.4 Supramolecular functionalization of SWNTs with conjugated polyelectrolytes

Anionic conjugated polyelectrolytes (CPEs), derivatives of polyphenylene (a-PP) and poly(phenylene ethynylene) (a-PPE) (shown in Figure 7) were found to interact strongly with SWNTs, presumably by  $\pi - \pi$  stacking. Unlike smaller species, such as pyrene and naphthalene derivatives, the CPE functionalized SWNTs did not precipitate even in the absence of free adsorbate. Raman spectroscopy studies indicate that these CPEs may preferentially complex smaller diameter SWNTs.

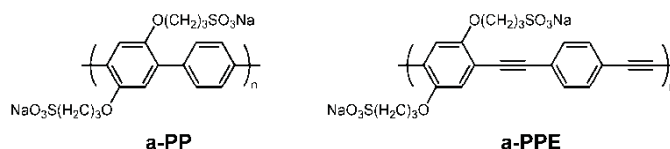


*Figure 7: Chemical structures of the two CPEs used for nanotube functionalization.*

### 2.4.1 Patterning of conjugated polyelectrolyte-functionalized SWNTs

Both of these structures were found to produce homogeneous solutions when mixed and sonicated with SWNTs, owing the conjugated backbone of these polymers, which enables the formation of strong  $\pi$ - $\pi$  stacking interactions with the surface of SWNTs. The anionic nature of the resulting nanotube-polymer complexes enables their patterning through electrostatic interactions with a pre-patterned surface. Patterned nanotube films were produced by directing the electrostatic adsorption of a-PP- and a-PPE-functionalized SWNTs on a pre-patterned, positively charged poly-4-vinyl-*N*-methylpyridine (PVMP) layer, which was produced via photochemical crosslinking, as previously described [5].

The optical profilometry image in Figure 8 depicts a regular 3D pattern of square features ( $90 \times 90 \mu\text{m}$ ) on the glass surface, exactly matching the openings of the TEM grid that was used as a photomask. Cross-sectional analysis indicated that the total height of these features was approximately 20 nm, with the crosslinked PVMP layer making up the majority of the observed features (Figure 8B). The transparent a-PP-SWNT layer was found to make up only the topmost approximately  $3 \pm 0.7$  nm, consistent with what is expected for a monolayer of individual polymer-functionalized nanotubes, or small bundles of these structures.

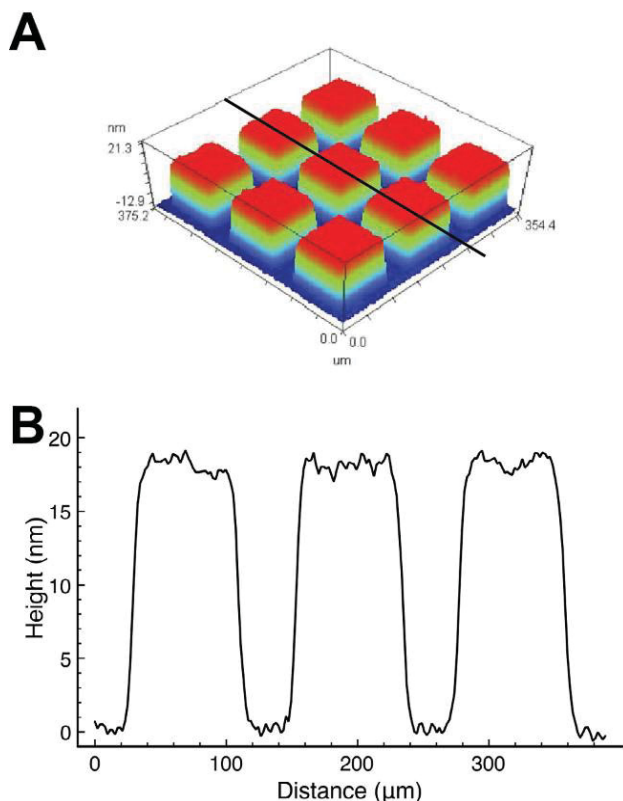


**Figure 8:** (A) Pattern of squares, imaged by optical profilometry, formed by immersing a pre-patterned glass slide with 90- $\mu\text{m}$  squares of cross-linked PVMP into an aqueous solution of a-PP-SWNTs. (B) Cross-sectional height vs. distance plot of the sample shown in (A), where the black line indicates the location of the cross section.

The exact nature of the deposited nanotube features was probed by scanning electron microscopy (SEM). Figure 9A depicts the pattern of square features that resulted from the photochemical crosslinking of PVMP followed by deposition of CPE-functionalized nanotubes. Clearly, the openings of the TEM grid are reproduced on the surface with high fidelity. Higher magnification images (Figure 9B) show that the interior of the squares, which are composed of the positively charged crosslinked PVMP layer below a layer of electrostatically deposited a-PP-SWNTs, indeed contain deposited nanotubes. A dense film of interwoven nanotubes is present in all areas that were initially irradiated and crosslinked during the photolithographic step (Figure 9C). Conversely, the trenches between the patterned squares, on which the PVMP was not crosslinked and therefore washed away, contained significantly fewer nanotubes, with only a small number of non-specifically adsorbed structures that were not successfully washed away during the rinsing step (Figure 9D).

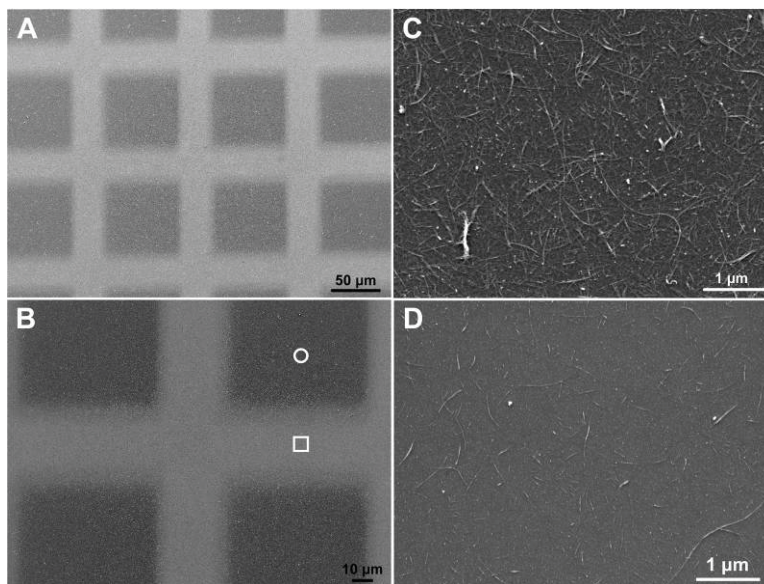


**Figure 9:** SEM images of patterned SWNTs on a glass substrate. A and B represent images of the substrate at two different magnifications, while C and D represent further magnified images of the areas marked with a white circle and square in image B, respectively.

#### 2.4.2 Electrophoretic deposition

Electrophoretic deposition involves the movement of charged species from solution onto the surface of an electrode in an applied electric field. In collaboration with the group of Prof. Igor Zhitomirsky, preliminary results on the electrophoretic deposition of CPE-functionalized SWNTs onto various electrode surfaces have been obtained (see Figure 10 for a schematic diagram of this process). It has been found that excellent deposits, with uniform and controllable thickness, can be prepared using this technique. Figure 11 shows several images of cross sections of electrophoretically deposited films on silicon substrates. From these images, it is clear that deposits can be produced, and exhibit easily controllable properties. We have also produced deposits on indium tin oxide surfaces that range in thickness from 80 nm to nearly 11 microns. This technique should be applicable to the deposition of nanotube coatings onto carbon felt used in the preparation of supercapacitors. This work is very preliminary, and deposition on carbon felt will be explored as a potential new direction of this project.

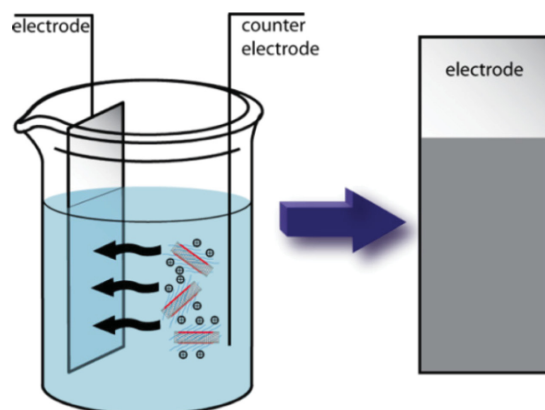


**Figure 10:** Schematic representation of electrophoretic deposition of appropriately functionalized carbon nanotubes onto an electrode surface.

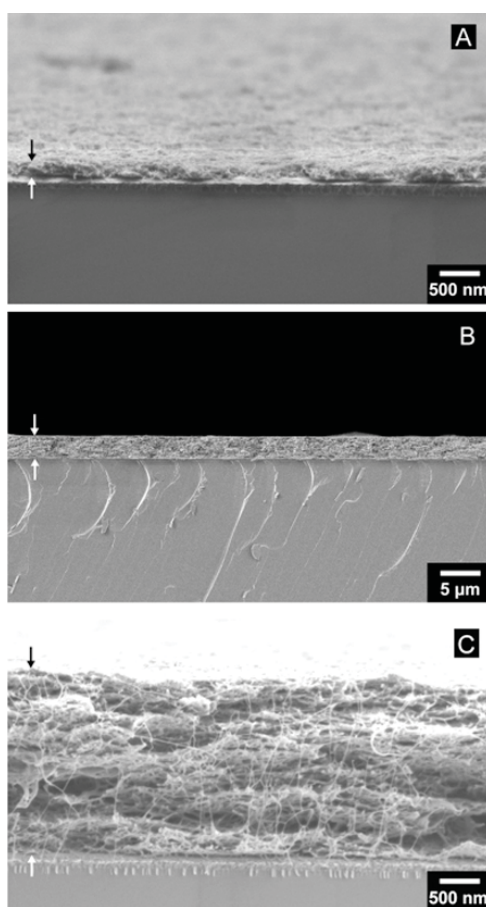


**Figure 11:** Electrophoretically deposited films of CPE-functionalized SWNTs. (A) Image of a relatively thin film of approximately 200 nm thickness; (B) Thicker film of approximately 2 micron thickness; (C) Close-up of the film in (B) showing the presence of nanotubes within the deposit.



## 2.5 Supramolecular functionalization of SWNTs with sulfonated polyaniline

In order to improve the electrical conductivity of the polymer – SWNT composites (and therefore the power density), sulfonated polyaniline (SPA) was investigated as the conjugated polymer for nanotube complexation. The resulting complexes exhibited significant improvement in both capacitance and conductivity (as evidenced by the current response and shape of the CV spectra, Figure 12).

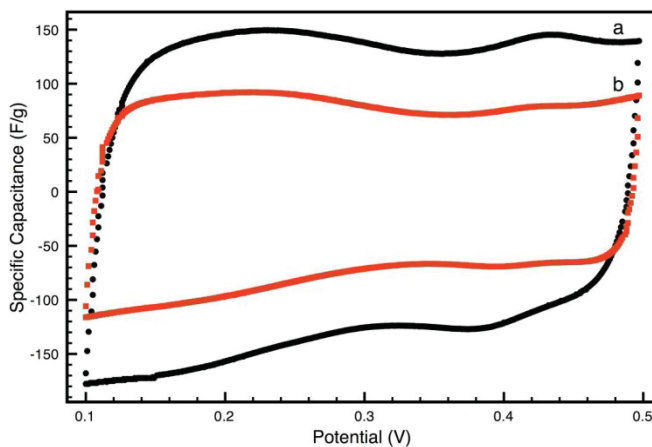


*Figure 12: Specific capacitance of SPA-SWNT (a) and SPA-MWNT (b).*

## 2.6 Results

Complexes between conjugated polymers and carbon nanotubes have been prepared and characterized. Polymer complexation can lead to the formation of highly stable solutions in a variety of solvents. This work illustrates that sonication of CNTs in the presence of appropriate polymers can effectively exfoliate the CNTs and stabilize against re-aggregation (see Figure 13).



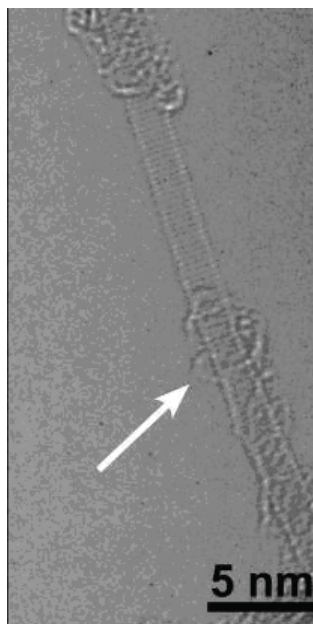


**Figure 13:** High resolution TEM (HRTEM) of a specimen reveals individual SWCNTs wrapped with polymer (see arrow).

Processible complexes exhibiting relatively high conductivity have been prepared using sulfonated polyaniline as the conjugated polymer. Although the sulfonated polyaniline is not as conductive as unmodified polyaniline, the sulfonation imparts solubility therefore processibility.

## 2.7 Conclusions

Complexes between conjugated polymers and carbon nanotubes can lead to the formation of highly stable nanotube solutions in a variety of solvents. These complexes have previously been characterized by UV-Vis, Raman, and Fluorescence spectroscopy. This work has been extended to the formation of complexes between carbon nanotubes and conjugated polyelectrolytes, which allow the formation of aqueous solutions of nanotubes. In addition, this allows the use of electrostatic interactions to pattern nanotubes on surfaces with high resolution. It has been demonstrated that conduction nanotube patterns of complex shape and micron dimensions can be easily prepared with simple, easily available equipment. In terms of carbon felt coatings for capacitor electrode fabrication, the aqueous solutions of CPE-SWNT complexes proved problematic because these solutions were not able to wet the hydrophobic carbon felt substrate. This problem has been resolved by preparing solutions of the same nanotube complexes in ethanol. It has also been found that the proton conducting polymer, Nafion, is effective in solubilising SWNTs in ethanol. This latter material is promising for the preparation of highly conductive electrodes for capacitor applications, and will be tested shortly.

## 2.8 Most significant results

1. Exploration of nanotube functionalization chemistry with conjugated polymers has led to the development of several polymer families that interact strongly with the nanotube surface. Through this work we compared covalent functionalization to supramolecular functionalization of SWNTs with identical polymer structures. We showed that covalent functionalization decreases nanotube conductivity by several orders of magnitude, even when a conjugated linker is used.
2. The interaction between conjugated polymers and nanotube surfaces is strong enough to allow removal of excess polymer from solution, which greatly simplifies characterization of the resulting materials. We showed that the polymer-nanotube interaction can be followed spectroscopically through a red-shift in polymer absorption, and a near-quantitative quenching of polymer fluorescence.
3. We showed that the same supramolecular functionalization chemistry could be extended to conjugated polyelectrolytes, enabling dissolution of SWNTs in aqueous solution. This allowed us to investigate the functionalization of nanotubes with highly conductive, self-doped polymers such as sulfonated polyaniline (SPA). Supercapacitor devices based on this polymer system were fabricated and tested, and were found to yield capacitance values of nearly 170 F/g (of active material in a single electrode configuration). The drawback to these devices was the difficulty in fabrication as the highly polar aqueous solutions do not easily penetrate the carbon felt electrode used to support the nanotubes. In addition, the overall conductivity of the nanotube materials has to be improved to increase capacitance values. To remedy both of these problems, we investigated other solvent systems and found that the CPE-nanotube complexes were also soluble in ethanol, which provides the right balance of hydrophilicity for the formation of stable solutions and hydrophobicity for infiltration of the carbon felt. In addition, we found that incorporation of the excellent proton conductor Nafion allowed formation of stable nanotube solutions, which should enhance overall conductivity.
4. Patterning of nanotube complexes by electrostatic interaction with an oppositely charged pre-patterned surface was also investigated and found to result in facile formation of intricate high-resolution (micron-scale) patterns without the need for expensive photolithography equipment. This work also led to preliminary investigation of electrophoretic deposition of nanotubes on electrode surfaces. Extension of this work to the deposition of nanotubes on carbon felt electrodes is therefore feasible and a promising direction for future studies.

### **3 Conducting polymer – carbon nanotube composites**

---

Research performed at the Dockyard Lab Pacific (DLP) focussed on conducting polymer – carbon nanotube composites, in which the carbon nanotubes are coated with a conducting polymer. Both parent materials exhibit double layer capacitance, however, conducting polymers are also capable of storing charge through redox reactions (pseudocapacitance). Thus the capacitance of conducting polymers is typically much larger than CNTs. Although the majority of the charge is stored by the CPs, one of the benefits of the composite is that it exhibits higher conductivity than the parent materials, presumably due to a reduction in contact resistance. This enhanced conductivity translates into higher power density. Moreover, the mechanical robustness of CNTs offers a scaffold that enhances the lifetime of the CPs, which possess poor mechanical properties. Furthermore, the use of CNTs as scaffolding may result in enhanced surface area and optimized porosity, yielding higher energy and power density than CPs alone.

#### **3.1 Purity and functionalization of CNTs**

There are several obstacles to effectively utilize CNTs: purity, defects, and high cohesive energy density. One of the first tasks was to determine a means to assess the quality of CNTs and to evaluate the information typically provided by suppliers. The findings were captured in a TM in which we evaluated the quality of a commercial source of MWCNTs with respect to purity and acid functionality [6]. Impurities typically found in CNTs (both SWCNTs and MWCNTs) are residual metal catalyst (from the preparation process) as well as amorphous and graphitic carbon formed during side reactions. The MWCNTs were qualitatively characterized by scanning electron microscopy (SEM) and transmission electron microscopy (TEM) in which non-nanotube (NT) carbon can be seen using both techniques; the TEM also provides qualitative information regarding metal content. The metal content was quantitatively determined by inductively coupled plasma mass spectrometry (ICP-MS), and the degree of surface acid functionality was determined by acid titration. Thermogravimetric analysis (TGA) was also used to characterize the material.

The next task undertaken was to address the purity issues that exist with almost all sources of CNTs. A purification protocol has been developed at DLP [7] [8] that removes the majority of residual metal catalyst and amorphous carbon (see Annex A). This protocol is straightforward, scalable, applicable to all sources of MWCNTs, and the progress of which can be monitored by TGA.

Intentional acid functionalization of the CNTs was also performed with a view to improving processing, and the effect on the polyaniline – nanotube (PAni-NT) composite electrical properties was assessed. Improved dispersion was observed, however, not unexpectedly, the functionalization was detrimental to the resulting electrical conductivity.<sup>8</sup> That said, some composites prepared with highly functionalized tubes did exhibit electrical conductivity on the same order as those without – presumably the detrimental effect was offset by improved dispersion. These findings warrant additional investigation.

## 3.2 Active material screening protocol

A means to screen a wide range of potential active materials was also developed. This method enabled a relatively quick evaluation of whether a material exhibited sufficient capacitance, and involves the preparation and measurements of electrodes in a half cell configuration immersed in 0.5M H<sub>2</sub>SO<sub>4</sub> (aq) [9]. This method enables the accurate measurement of chemically prepared active material. Three measurement techniques, cyclic voltammetry (CV), constant current charge-discharge, and electrochemical impedance spectroscopy (EIS), were employed to ensure the accuracy and consistence of the data (see Table 2); replicate electrodes were measured to ensure reproducibility of electrode preparation (see Figure 14).

**Table 2:** Capacitance values for the same electrode made with PANi-2NSA/MWCNT, based on different measurement methods.

Method	Capacitance (F/g)
EIS	128
CV	152
Constant Current Charge-Discharge	152

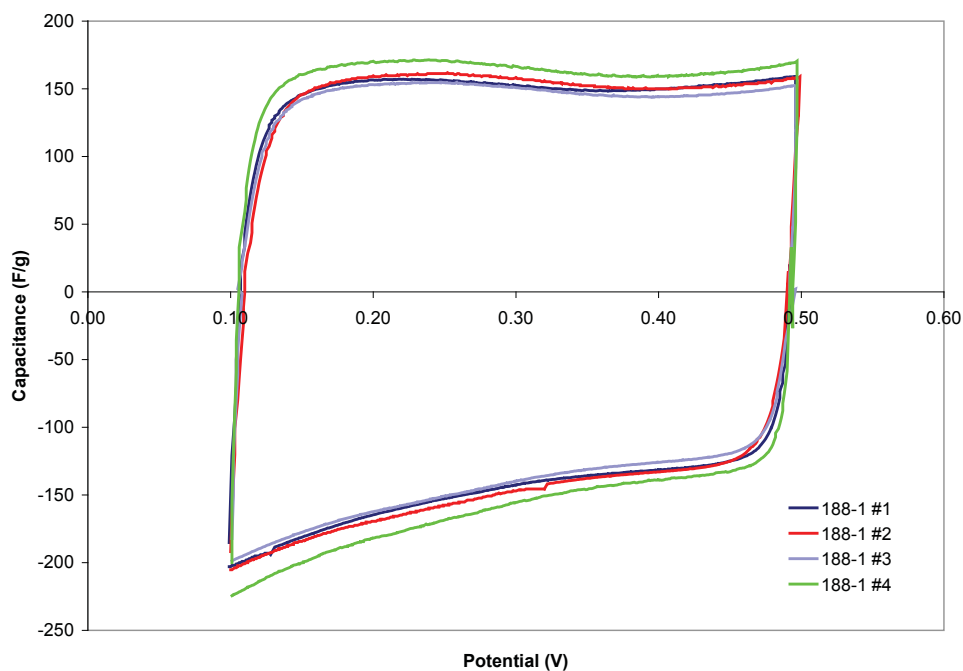


**Figure 14:** Cyclic voltammetry data demonstrate the reproducibility of the electrode preparation (scan rate 10 mV/s).

This method of preparing electrodes was found to be sufficiently accurate for electrodes having an active material mass of approximately 1 mg. If the active material mass is much less than 1 mg, then the relative uncertainty of the mass ( $\pm 0.02$  mg) becomes large. If the active material mass is much larger than 1 mg then the resistance of the material (either electronic or ionic) results in distorted CV spectra (rice grain shape), and hinders accurate determination of the capacitance.

The next step in the screening protocol is to develop a method by which larger quantities of active materials can be used, without the resistance hampering measurement, to allow for accurate power density measurements to be made. With small active material quantities ( $\sim 1$ mg) the measurement of the power density is limited by the inability of the small amount of material to handle large currents (and the power density is proportional to the applied current).

### 3.3 The effect of dopant on capacitance

Corroborating the literature, previous research performed at DLP has determined that the size and shape of the dopant has an effect on the conductivity of polyaniline [10]. As the dopant increases in size, the conductivity of the polymer is found to decrease (see Figure 15). This is attributed to the morphology of the polymer; the dopant anions are closely associated with the protonated imine sites on the backbone chain (Figure 16), thus the size and shape of the dopant affects how the polymer packs.

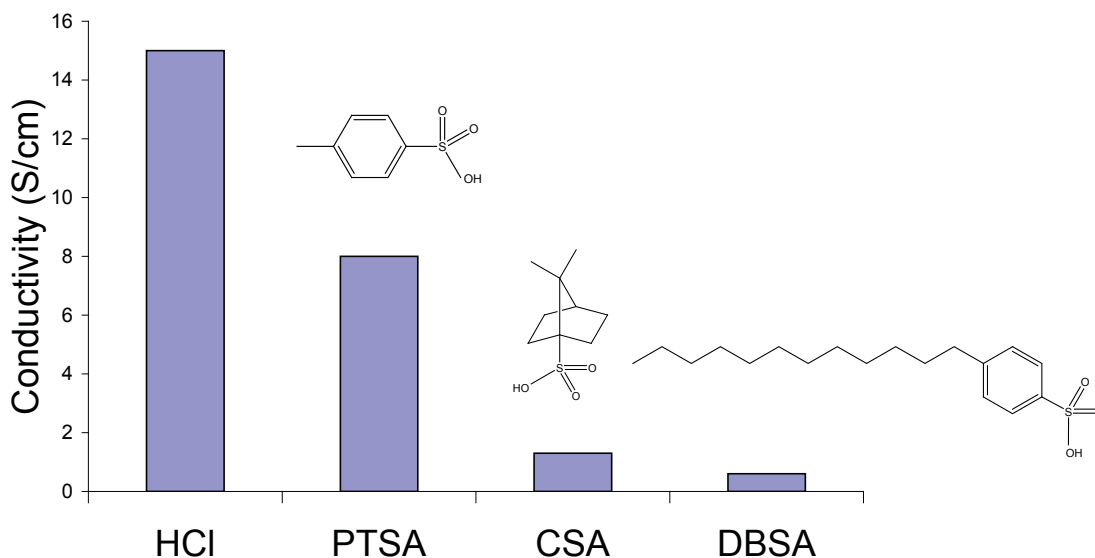


**Figure 15:** DC conductivity for polyaniline doped with acids (dopants) of varying size and shape.

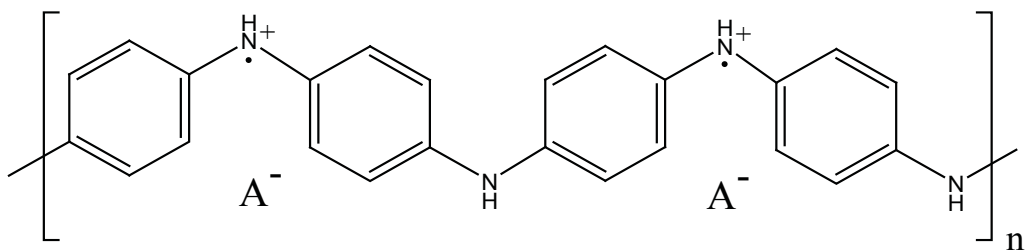


**Figure 16:** A repeat unit for doped polyaniline, in which the dopant anion is represented as  $A^-$ .

For conducting polymers there are two contributions to the dc conductivity of conducting polymers: the intrachain conductivity (conductivity along a polymeric chain) and the interchain conductivity (charge hopping from one chain to a neighbouring chain).

For polyaniline the major contributor is the interchain conductivity, in which the charge hops from one chain to another. Thus, the larger the dopant, the farther apart the neighbouring chains, thus the lower the conductivity.

The ability to tailor the morphology of the polymer may translate into optimizing its porosity for charge storage purposes. To investigate this possibility, polyaniline – NT composites were prepared with three dopants of differing size and shape, and the capacitance measured. Figure 17 shows the structure of the dopants (*p*-toluenesulfonic acid (PTSA), dodecylbenzenesulfonic acid (DBSA), and 2-naphthalenesulfonic acid (2-NSA) as well as TEM images of these composites (each contains 42% CNTs by mass).

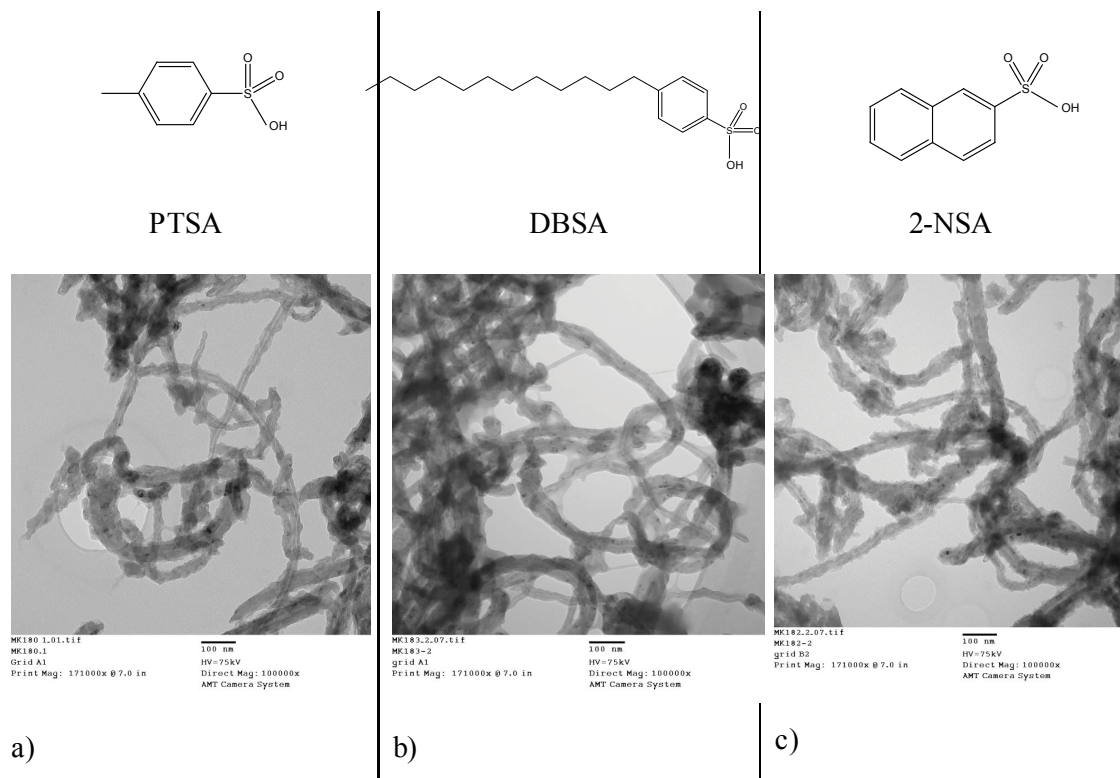


**Figure 17:** Dopant structure and transmission electron microscope (TEM) images of MWCNTs coated with a) PAni-PTSA, b) PAni-DBSA, and c) PAni-2NSA.

The capacitance of each composite was measured and normalized with respect to the mass of the polyaniline backbone chain (to account for the difference in dopant molar mass) (see Figure 18).

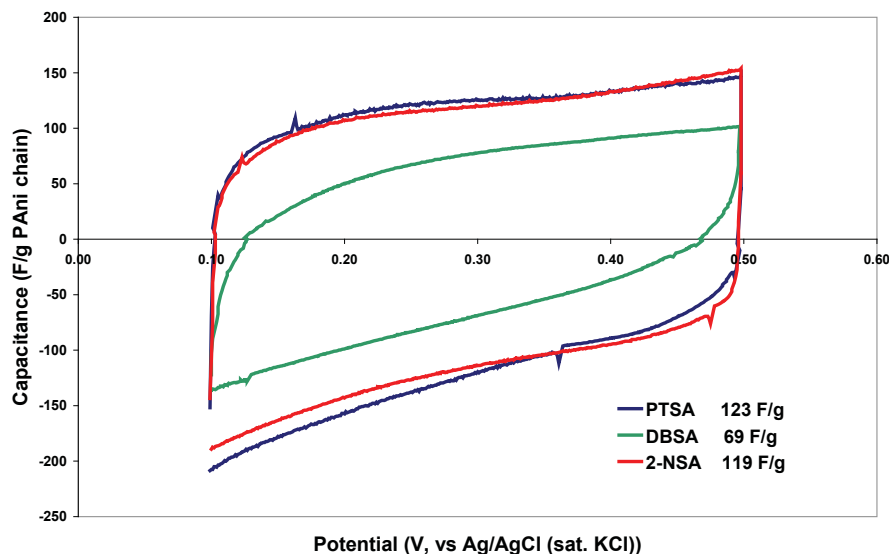


**Figure 18:** Cyclic voltammogram showing capacitance as a function of potential for PANi/PTSA-MWCNT, PANi/DBSA-MWCNT, and PANi/2-NSA-MWCNT. All materials contain ~ 42% MWCNT. The capacitance has been normalized to exclude dopant mass.

The highest capacitances were achieved with the composites doped with PTSA and 2-NSA, however the rough, but uniform morphology of the PANi/2-NSA on the MWCNTs looked promising, and warranted further investigation.

A series of PANi/2-NSA-MWCNTs composites were prepared with varying polymer content, with both thin (10 nm diameter) and thick (30 – 50 nm diameter) MWCNTs. PANi/2-NSA alone exhibits a capacitance of approximately 300 F/g, whereas the MWCNTs exhibit capacitances of 16 and 70 F/g, for the thick and thin MWCNTs, respectively. Polyaniline exhibits higher capacitance than the CNTs, as it can also store charge via a redox storage mechanism known as pseudocapacitance,  $C_p$ . As the polymer content was increased along the series, the capacitance of the composite was also found to increase almost monotonically (Figure 19), although it was anticipated that some compositions would exhibit higher capacitance than the polyaniline alone. The absence of an enhancement was unexpected as there are a number of reports in the literature in which polyaniline – CNT composites exhibit greater capacitance than the polyaniline alone [11] [12] [13]. If the polymer packs in such a way that renders the interior of a particle inaccessible to the electrolyte, then it is reasonable to expect that a larger proportion of polymer is accessible when the same quantity is supported on a high surface area scaffold. It is reasonable to expect that better accessibility should result in greater capacitance.



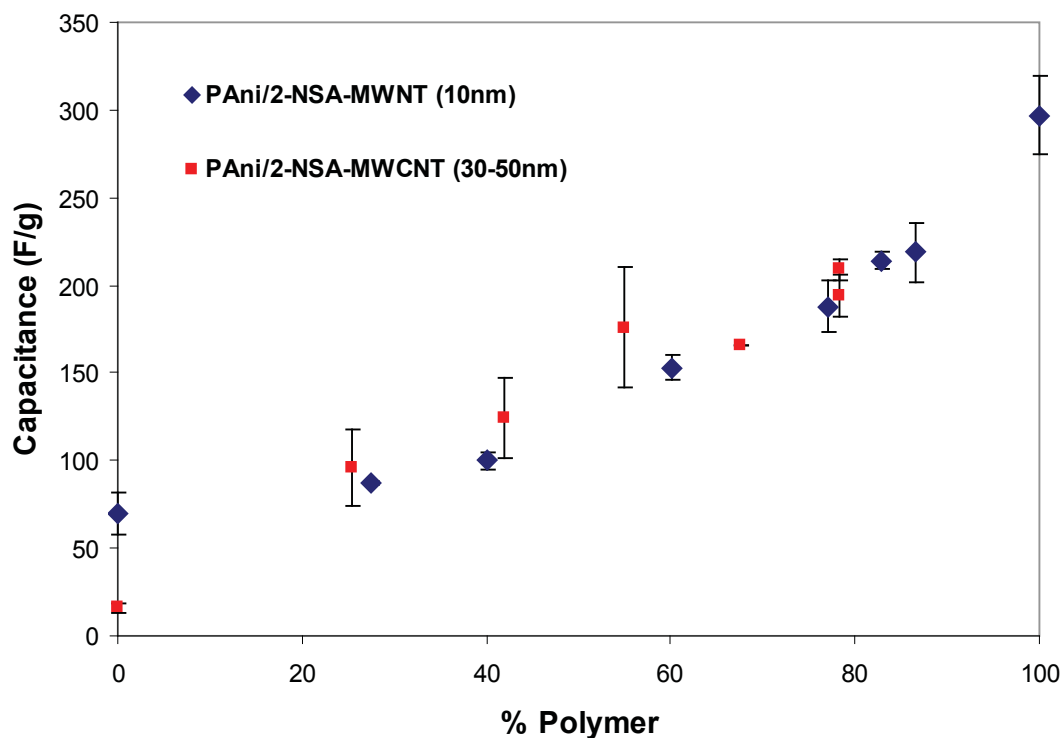


**Figure 19:** Plot of capacitance versus polymer content for PAni/2-NSA-MWCNT composites using both thin (10 nm diameter) and thick (30 – 50 nm diameter) MWCNTs.

The dependence of the capacitance on polymer content alone, and not on the CNT dimensions is rather poignant. The surface area of CNTs is inversely proportional to the diameter, thus the scaffold surface area would be expected to affect the capacitance, if the surface area were fully exploited. The data indicate that full surface exploitation has not been achieved.

When initial attempts did not yield the expected enhancement, it was thought that perhaps significant polymerization in bulk solution had occurred giving rise to a large proportion of polymer that was inaccessible to electrolyte. To address this, a series of composites were prepared in which very low concentrations of monomer were used, to minimize polymerization in bulk solution, and the polymer was built up in an iterative fashion. After each synthetic iteration the product was isolated and then used as the starting material for the next iteration. The capacitance of the final products of the iterative approach did not exhibit an enhancement (see Figure 20).

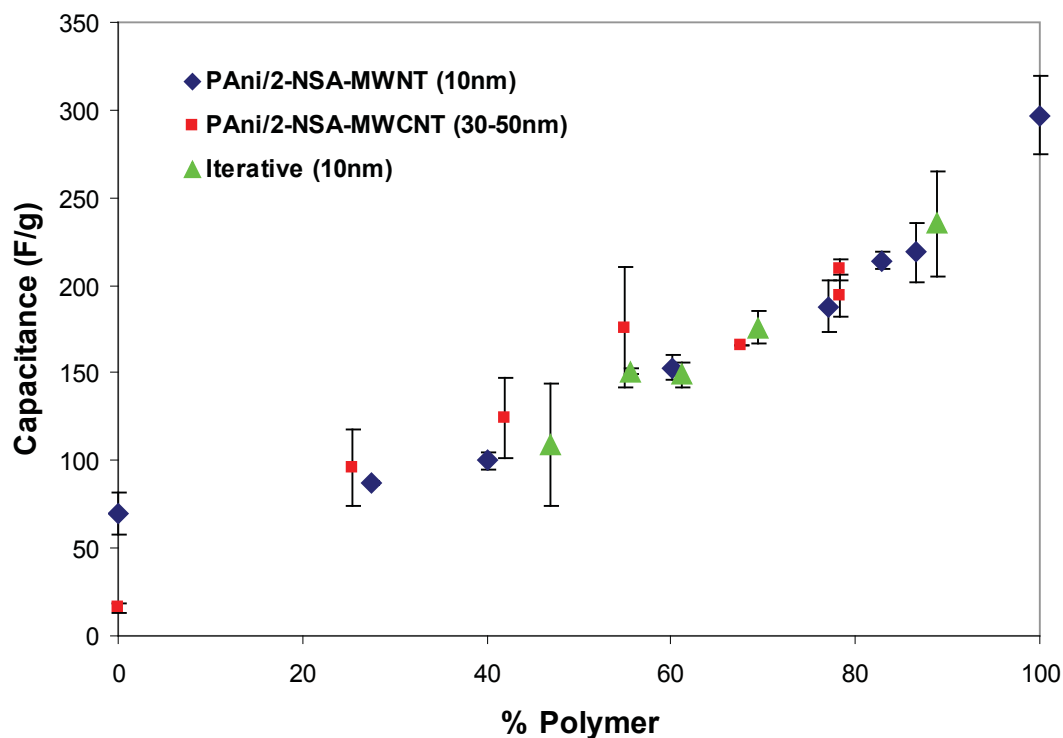


**Figure 20:** Plot of capacitance versus polymer content for PANi/2-NSA-MWCNT composites prepared by the standard protocol, as well as using by utilizing a synthetic iteration approach.

If the MWCNTs were not fully dispersed, and were aggregated to some degree, then the surface area may not be wholly available for exploitation. It was considered whether poor dispersion may have played a role in the absence on an observed enhancement. Composites were prepared in which the CNTs were dispersed for longer periods of time, however the products did not exhibit an enhancement (see Figure 21).

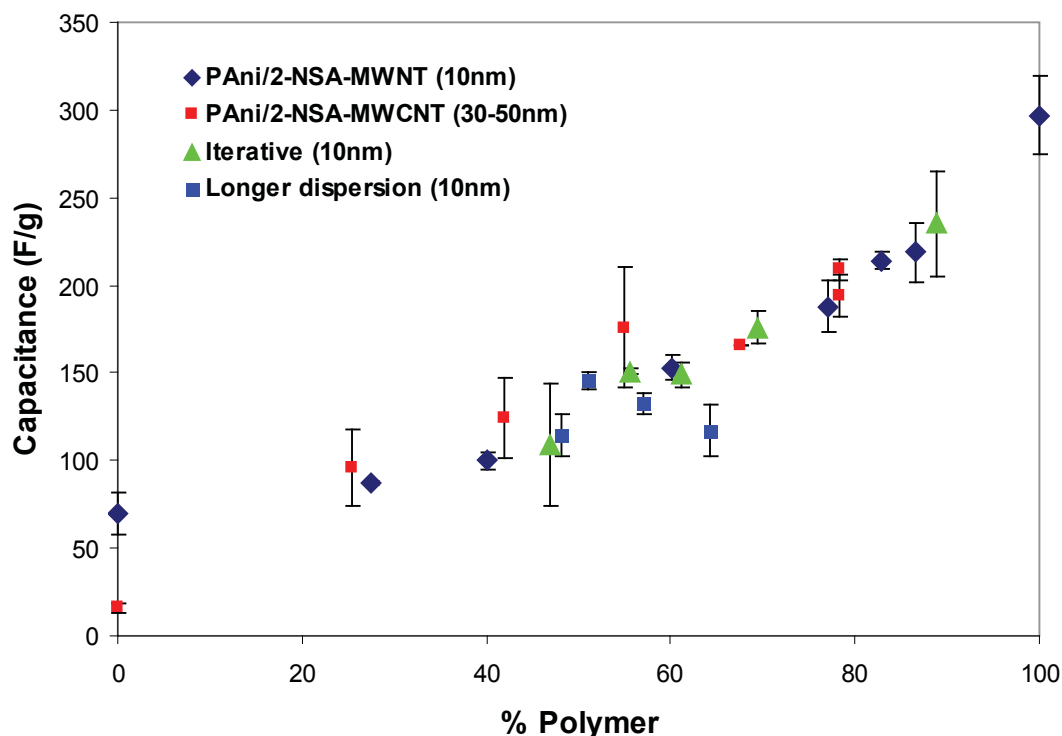


**Figure 21:** Plot of capacitance versus polymer content for PANi/2-NSA-MWCNT composites prepared by the standard protocol, as well as using an iterative approach, and dispersing the MWCNTs for a longer period of time.

The variation in CNT diameter, and therefore surface area, did not result in an enhancement, nor did the iterative synthetic approach or the extended sonication time. In fact, the measured capacitances were very close to those prepared by the standard protocol. Within experimental uncertainty, the capacitance increased with polymer content linearly, and in fact the data appear to roughly follow a rule of mixtures. This correlation would indicate very strongly that the polymer chains were indeed accessible to the electrolyte in the polymer alone.

This is in contrast to reports in the literature, however, the morphology of the polyaniline employed here from that reported in the literature. The polyaniline in literature was doped with relatively small dopants, such as hydrochloric acid (HCl), nitric acid (HNO<sub>3</sub>), and sulphuric acid (H<sub>2</sub>SO<sub>4</sub>) [12] [13] [14]. It is reasonable to conclude that the spacing between polyaniline chains in these polymers is relatively small, thus the chains in the interior of particles would be expected to be less accessible to electrolyte. It would appear that the use of a large dopant such as 2-NSA gives rise to a more porous structure, facilitating electrolyte mobility.

### 3.4 Conclusions

This project provided the opportunity for a large-scale purification protocol to be developed for MWCNTs of varying diameter. This purification method utilizes common laboratory equipment

and a thermogravimetric analyzer (TGA) to assess the state of purity. The effect of MWCNT acid functionality was also assessed with respect to capacitance. Although the surface functionality is detrimental to conductivity, it facilitates dispersion, and does not appear to negatively impact capacitance.

The screening protocol provides a fairly quick but accurate assessment of the capacitance of small quantities (~ 1 mg) of active material. Furthermore, the shape of the CV curve provides qualitative information on the resistance of the active material, as well as the pseudocapacitance. Work is presently underway to measure larger quantities of active material, thus permitting accurate power density measurement.

The capacitance of PANi-MWCNT composites is dependent on the composition of the polyaniline, which can be tailored to optimize the surface characteristics.

### **3.5 Most significant results**

The most significant result is the effect of the dopant structure (size and shape) on the capacitance of polyaniline. The ability to tailor the polymer structure to optimize surface area and porosity is the key to optimizing the capacitance of conducting polymers. Studies are currently underway to better understand the structure-property relationships between the polyaniline, specifically the nature of the dopant, and the surface properties and capacitance.

## 4 Ruthenium oxide – carbon nanotube composites

---

In addition to conducting polymers, redox active metal oxide species can be deposited onto MWCNTs for enhanced capacitance. Collaboration with the Pickup group at Memorial University focussed on the synthesis and characterization of ruthenium oxide MWCNT composites.

### 4.1 Synthesis and characterization

Nanoparticles of ruthenium oxide were deposited onto MWCNTs via a process in which high oxidation state ruthenium (Ru(VI) and Ru(VII)) were reduced on the surface of the MWCNTs. The resulting ruthenium (Ru(IV)) precipitates on the surface in the form of a hydrous hydroxide/oxide, hereinafter referred to as ruthenium oxide (Ru oxide). Both purified (p-MWCNTs) and intentionally acid-functionalized MWCNTs (a-MWCNTs) were used in the synthesis of the composites to investigate whether a more oxidized MWCNT surface (acid-functionalized) had any effect on the composite properties. Energy dispersive X-ray spectroscopy (EDS) confirmed the presence and approximate loading of the ruthenium, 25% for p-MWCNT composites, and 16% for a-MWCNT composites. TEM images provided distribution and particle size information, and CV was used to evaluate capacitance [14].

The deposition of nanoparticles of ruthenium oxide, in the range of 1 – 3 nm, is evident in the TEM image of Ru oxide/p-MWCNTs shown in Figure 22; the Ru oxide appears to form in clusters in various locations of the MWCNTs. In contrast, the use of a-MWCNTs results in poorer dispersion of Ru oxide, and the particles exhibit a wider diameter range (Figure 23). Furthermore, the appearance of the a-MWCNTs is different from the p-MWCNTs, presumably due to the presence of surface functionalization at the start of the deposition process. The composite of a-MWCNT appears to have smears of amorphous carbon present; it is not clear whether this would result from the additional MWCNT oxidation that occurs concomitantly with ruthenium reduction, or whether it was present initially.

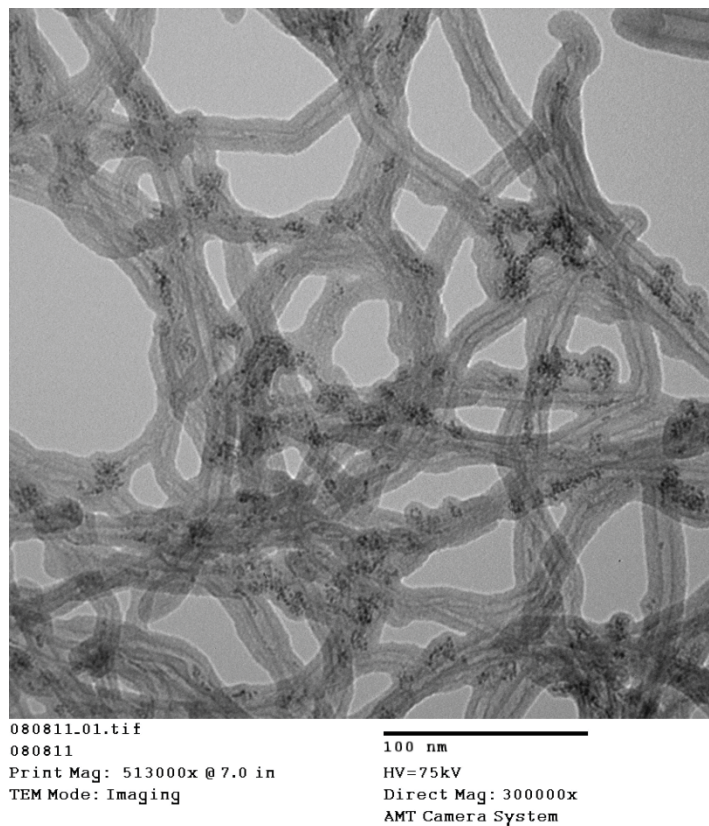


**Figure 22:** TEM of a 25.1% Ru oxide/p-MWCNT composite.

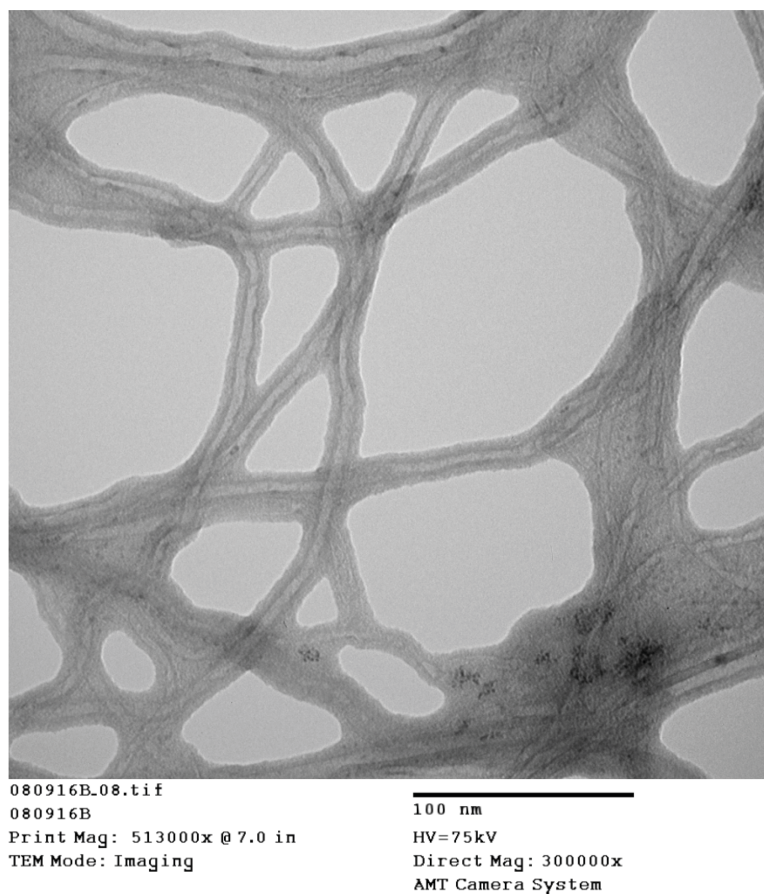


**Figure 23:** TEM of a 15.6% Ru oxide/a-MWCNT composite.

The CVs of the p-MWCNTs and a-MWCNTs are shown in Figure 24; the average capacitance of the purified MWCNTs is  $48.8 \pm 1.3$  F/g, whereas that of the acid-functionalized is  $69.0 \pm 1.4$  F/g. The increase of approximately 40% is due primarily to the presence of quinone-type functionality, exhibiting a pseudocapacitive peak at approximately +0.4 V vs. Ag/AgCl.

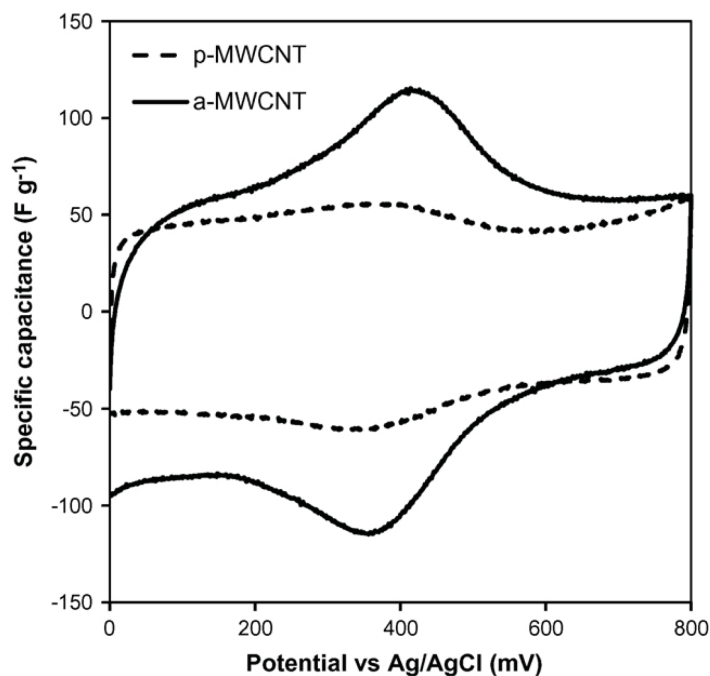


**Figure 24:** Cyclic voltammograms at  $20 \text{ mV s}^{-1}$  of p-MWCNT and a-MWCNT.

The specific capacitance of the composites, as determined by CV, was compared to that of the pertinent MWCNTs, Figure 25 and 26. The specific capacitance of the Ru oxide component was determined by accounting for the Ru oxide loading in the composite; the specific capacitance of Ru oxide was determined to be  $700 \pm 62 \text{ F/g}$ , and  $800 \pm 72 \text{ F/g}$  in the p-MWCNT and a-MWCNT composites, respectively. These values are not significantly different given the uncertainty in the values.



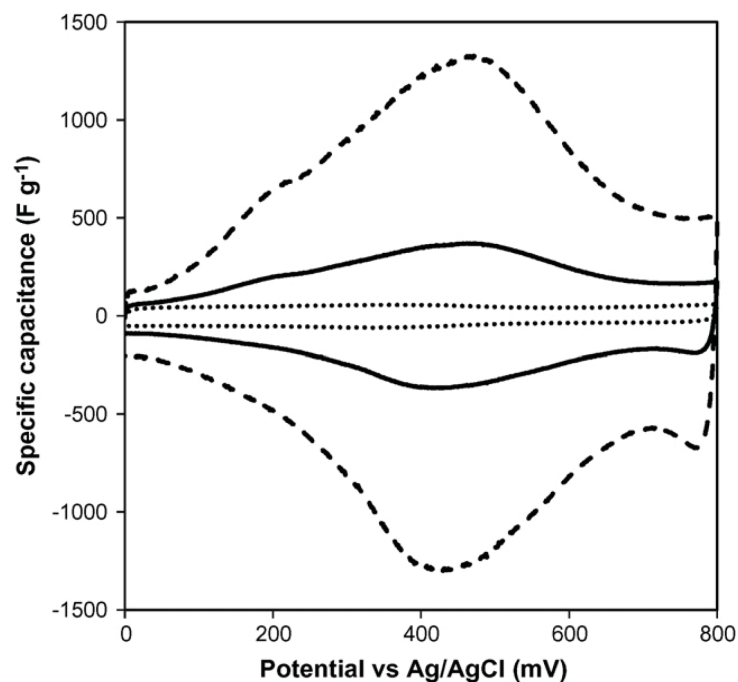


**Figure 25:** Cyclic voltammograms at  $20 \text{ mV s}^{-1}$  for 25.1 % Ru oxide/p-MWCNT (solid), blank p-MWCNT (dotted) and the calculated specific capacitance of the Ru oxide component of the composite (dashed).

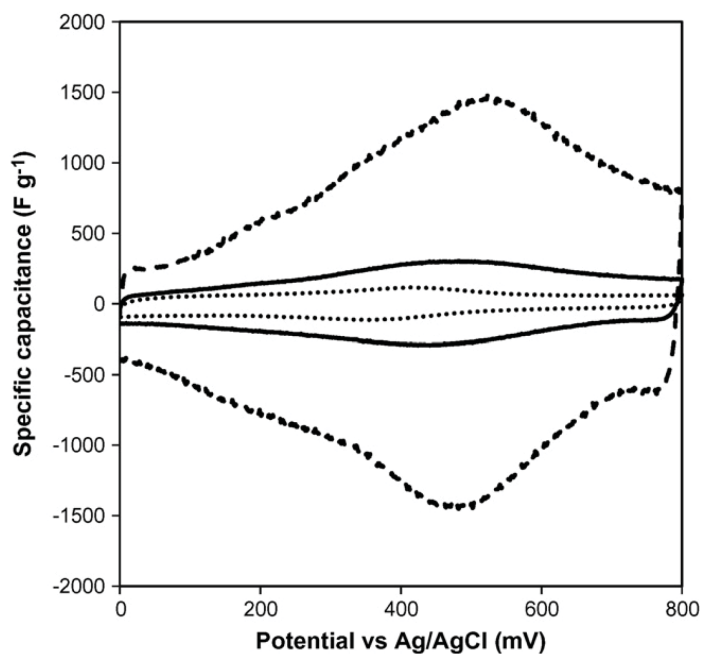


**Figure 26:** Cyclic voltammograms at  $20 \text{ mV s}^{-1}$  for 15.6 % Ru oxide/a-MWCNT (solid), blank a-MWCNT (dotted) and the calculated specific capacitance of the Ru oxide component of the composite (dashed).

A full cell was prepared in which both electrodes (symmetric cell) were comprised of the Ru oxide/p-MWCNT composite. The CV spectrum measured at 50 mV/s indicates fast switching, as evidenced by the quick response of the current (nearly vertical CV spectrum shape) in the vicinity of the potential limits (Figure 27). Fast switching corresponds to lower resistance, thus fast charging and discharging. Higher charge and discharge rates mean greater power density.

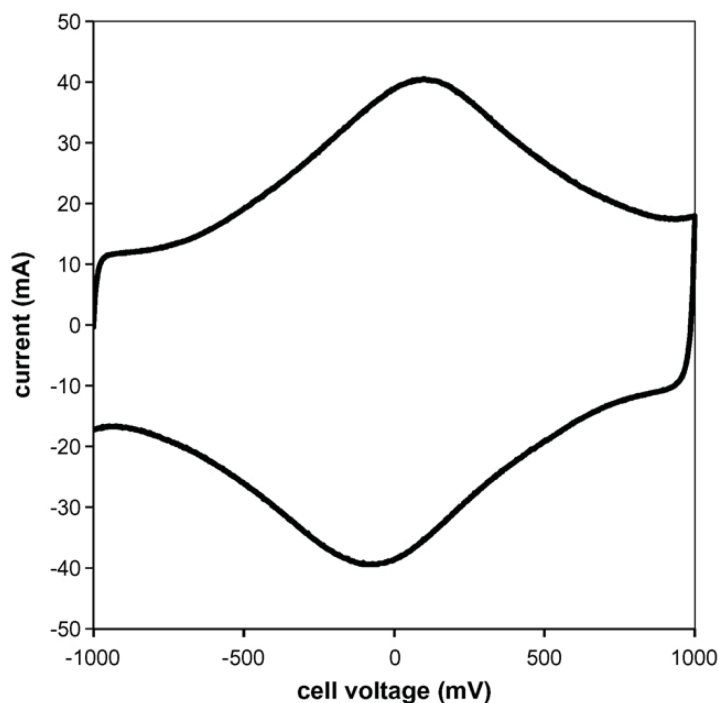


**Figure 27:** Cyclic voltammogram at  $50 \text{ mV s}^{-1}$  of a full cell of 25.1% Ru oxide/p-MWCNT. Each electrode was comprised of approximately 5 mg of active material.

Longer term testing of the full cell comprised continuous charging and discharging between 0 and 1V at a constant current of  $100 \text{ mA/cm}^2$ . The constant current charge and discharge times were plotted against cycle number (Figure 28), and it is readily evident that the time, and therefore capacitance, increases with time, and remains steady over 20 000 cycles. This increase in capacitance is likely due to an increase in accessible active sites, as the electrolyte penetrates into the small pores of the active material.

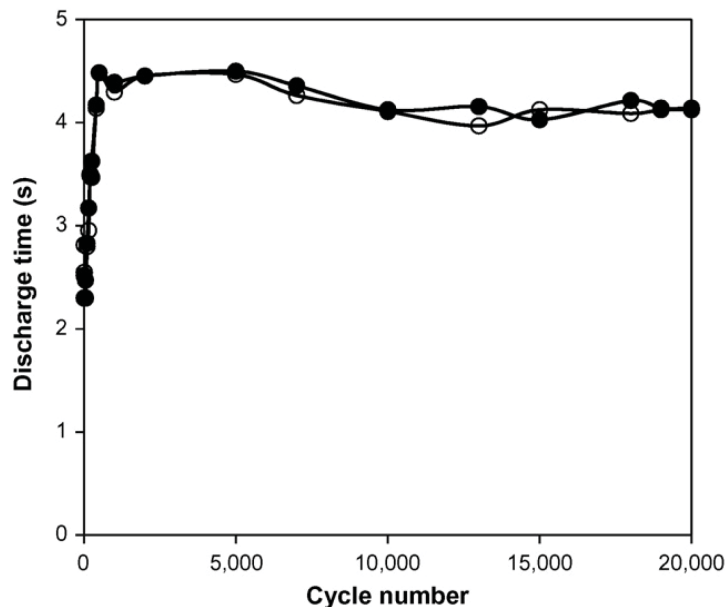


**Figure 28:** Charging (○) and discharging (●) times between 0V and 1V at a rate of 100 mA/cm<sup>2</sup>. Note the initial increase in time and the stability up to 20 000 cycles.

At 100 mA/cm<sup>2</sup>, the discharge rate employed here, the energy and power densities for the 1,000th cycle of the 25.1 % Ru oxide/p-MWCNT supercapacitor were 4.3 Wh kg<sup>-1</sup> and 3.3 kW kg<sup>-1</sup>, respectively. These values show promise, but it is important to note that the power density is dependent on discharge rate, which is limited by the quantity of active material. To accurately determine the maximum power density of this active material, fabrication of cells that are large enough to mitigate limitations due to loading, is critical.

## 4.2 Conclusions

A novel synthesis of Ru oxide/p-MWCNT composites and their electrochemical characterization is reported here. The materials demonstrated excellent performance in full cell configuration, with high specific capacitances, low resistances, and outstanding durability. The composites exhibit much higher capacitances than the nanotubes alone, with the Ru oxide component contributing an impressive specific capacitance of 803±72 F/g.

## 4.3 Most significant results

The high energy storage capacity of Ru oxide can be exploited by distributing this material as nano-sized particles onto high surface area MWCNTs. The Ru oxide component contributes significantly to the overall capacitance, as evidenced by the enhancement in storage capacity over and above that of the nanotubes alone. The performance of a full cell configuration is highly dependent on the electrical resistance of each component and interface. Thus minimizing the

resistance in the assembly of the full cell, for example through compression to minimize contact resistance, is important to the overall performance.

It is important to note that the power density of a material or of a cell is dependent on the quantity of active material. Cells having small quantities of active material are naturally limited in their performance due to an inherent inability to handle high current density. With more active material, the cell can handle higher current density. However, there is a limit, as the electrical resistance also increases, resulting in a maximum current density, and therefore power density.

## **5 Conclusions and future work**

---

Attempts to prepare devices to evaluate scalability as well as facilitate power density measurements (cannot be done adequately on lab scale, since power density is dependent on current applied, and on lab scale only a small amount of current can be applied).

In order to accurately determine power density, full cell prototype devices must be optimized. There are a several aspects to prototype assembly and optimization of the different components and how they are put together must be investigated to ensure that the overall device is optimized.

Although the active material may be well-characterized in small amounts on the lab-scale, the full potential of the material cannot be realized until it has been incorporated into a fully optimized system.

This page intentionally left blank.

## References

---

- [1] Andrukaitis, E.; Bock, D.; Eng, S.; Gardner, C.; Hill, I. Technology Trends, Threats, Requirements, and Opportunities (T<sup>3</sup>R&O) Study on Advanced Power Sources for the Canadian Forces in 2020, Defence R&D Canada, 2001
- [2] Peigney, A.; Laurent, C.; Flahaut, E.; Bacsá, R. R.; Rousset, A. Carbon **2001**, 39, 507-514
- [3] Li, HM and Adronov, A, Carbon 2007, 984-990
- [4] Cheng, F. Y.; Adronov, A. Chem. Mater. **2006**, 18, 5389-5391
- [5] Xu, H.; Hong, R.; Wang, X.; Arvizo, R.; You, C.; Samanta, B.; Patra, D.; Tuominen, M. T.; Rotello, V. M. Adv Mater **2007**, 19, 1383-1386
- [6] M.C. Kopac and T.A. Huber, Assessing the Quality of Carbon Nanotubes, DRDC Atlantic TM 2007-136, Unclassified, April 2007
- [7] Huber, T. A.; Kopac, M. C.; Chow, C. (2008), The quantitative removal of metal catalyst from multi-walled carbon nanotubes with minimal tube damage, Can. J. Chem., 86 (12), 1138 – 1143
- [8] C. Chow and T. Huber, The Potential of Conducting Polymer – Carbon Nanotube Composites as Supercapacitor Electrodes, Unclassified, DRDC Atlantic TM 2007-320, October 2007
- [9] T.A. Huber, M.C. Kopac, F. Wong, Screening Protocol for the Electrochemical Characterization of Potential Supercapacitor Materials, Unclassified, DRDC Atlantic TM 2009-279, November 2009
- [10] T. Huber, P. Saville, D. Edwards, Investigations into the Polyaniline and Polypyrrole Families of Conducting Polymers for Application as Radar Absorbing Materials, Unclassified, DRDC Atlantic TM2003-005, January 2003
- [11] Gupta, V. and Miura, N., J. Power Sources, **157**, 616-620 (2006)
- [12] Zhou, Y. -K., He, B. -L., Zhou, W. -J., Huang, J., Li, X. -H., Wu, B., Li, H. -L., Electrochimica Acta, **49**, 257-262 (2004)
- [13] Zhou, Y.-K., He, B.-L., Zhou, W.-J., Li, H.-L., J. Electrochem. Soc., **151**, A1052-A1057 (2004)
- [14] X. Liu, T.A. Huber, M.C. Kopac, and P.G. Pickup, Electrochimica Acta, 2009, 54, 7141-7147

This page intentionally left blank.



## List of symbols/abbreviations/acronyms/initialisms

---

A	area
a-MWCNTs	acid-functionalized MWCNTs
C	capacitance
cm	centimeter
CNT(s)	carbon nanotubes
CP	conducting polymer
CPE	conjugated polyelectrolytes
CV	cyclic voltammetry
d	distance or thickness of material
3D	three dimensional
DBSA	dodecylbenzenesulfonic acid
DE	directed energy
DLP	Dockyard Lab Pacific
DND	Department of National Defence
DRDC	Defence Research and Development Canada
DSTKIM	Director Science and Technology Knowledge and Information Management
EDLC	electrochemical double layer
EDS	energy dispersive X-ray spectroscopy
EIS	electrochemical impedance spectroscopy
F	Farad
g	gram
HCl	HCl(aq), hydrochloric acid
HNO <sub>3</sub>	nitric acid
H <sub>2</sub> SO <sub>4</sub>	sulfuric acid
HRTEM	high resolution transmission electron microscopy
ICP-MS	inductively coupled plasma – mass spectrometry
KE	kinetic energy
kg	kilogram
L	litre
LAV	light armoured vehicles
nm	nanometer
mA	milliamp

MEM	micro electro mechanical
mg	milligram
$\mu\text{m}$	micron (micrometer)
mV	millivolt
MW	megawatt
mW	milliwatt
MWCNT(s)	multi-walled carbon nanotubes
2-NSA	2-naphthalenesulfonic acid
PAni	polyaniline
PF	polyfluorene
PFT	poly(fluorene-co-thiophene)
PP	polyphenylene
PSS	poly(styrene sulfonate)
PTSA	<i>p</i> -toluenesulfonic acid
PVMP	poly-4-vinyl- <i>N</i> -methylpyridine
R&D	Research & Development
RF	radio frequency
Ru oxide	ruthenium oxide
s	second
$\sigma$	sigma, conductivity
SEM	scanning electron microscopy
SPA	sulfonated polyaniline
SWNT(s)	Single-walled carbon nanotube(s)
TEM	transmission electron microscopy
TGA	thermogravimetric analysis
TIF	Technology Investment Fund
TM	Technical Memorandum
UAV	unmanned aerial vehicles
UV-Vis	ultraviolet-visible spectroscopy
V	voltage
W	watt

DOCUMENT CONTROL DATA		
(Security markings for the title, abstract and indexing annotation must be entered when the document is Classified or Designated)		
1. ORIGINATOR (The name and address of the organization preparing the document. Organizations for whom the document was prepared, e.g., Centre sponsoring a contractor's report, or tasking agency, are entered in Section 8.)  Defence Research and Development Canada – Atlantic 9 Grove Street P.O. Box 1012 Dartmouth, Nova Scotia B2Y 3Z7		2a. SECURITY MARKING (Overall security marking of the document including special supplemental markings if applicable.)  UNCLASSIFIED
		2b. CONTROLLED GOODS  (NON-CONTROLLED GOODS) DMC A REVIEW: GCEC DECEMBER 2012
3. TITLE (The complete document title as indicated on the title page. Its classification should be indicated by the appropriate abbreviation (S, C or U) in parentheses after the title.)  Novel functionalized carbon nanotube supercapacitor materials : Contribution to the supercapacitor TIF		
4. AUTHORS (last name, followed by initials – ranks, titles, etc., not to be used)  Huber, T.		
5. DATE OF PUBLICATION (Month and year of publication of document.)  August 2014	6a. NO. OF PAGES (Total containing information, including Annexes, Appendices, etc.)  52	6b. NO. OF REFS (Total cited in document.)  14
7. DESCRIPTIVE NOTES (The category of the document, e.g., technical report, technical note or memorandum. If appropriate, enter the type of report, e.g., interim, progress, summary, annual or final. Give the inclusive dates when a specific reporting period is covered.)  Scientific Report		
8. SPONSORING ACTIVITY (The name of the department project office or laboratory sponsoring the research and development – include address.)  Defence Research and Development Canada – Atlantic 9 Grove Street P.O. Box 1012 Dartmouth, Nova Scotia B2Y 3Z7		
9a. PROJECT OR GRANT NO. (If appropriate, the applicable research and development project or grant number under which the document was written. Please specify whether project or grant.)  12sz07	9b. CONTRACT NO. (If appropriate, the applicable number under which the document was written.)	
10a. ORIGINATOR'S DOCUMENT NUMBER (The official document number by which the document is identified by the originating activity. This number must be unique to this document.)  DRDC-RDDC-2014-R63	10b. OTHER DOCUMENT NO(s). (Any other numbers which may be assigned this document either by the originator or by the sponsor.)	
11. DOCUMENT AVAILABILITY (Any limitations on further dissemination of the document, other than those imposed by security classification.)  Unlimited		
12. DOCUMENT ANNOUNCEMENT (Any limitation to the bibliographic announcement of this document. This will normally correspond to the Document Availability (11). However, where further distribution (beyond the audience specified in (11) is possible, a wider announcement audience may be selected.)  Unlimited		

13. **ABSTRACT** (A brief and factual summary of the document. It may also appear elsewhere in the body of the document itself. It is highly desirable that the abstract of classified documents be unclassified. Each paragraph of the abstract shall begin with an indication of the security classification of the information in the paragraph (unless the document itself is unclassified) represented as (S), (C), (R), or (U). It is not necessary to include here abstracts in both official languages unless the text is bilingual.)

Numerous functionalized carbon nanotube materials, utilizing a variety of means, were prepared and characterized with respect to their charge storage capability. These materials exploit the high surface area and dc conductivity of carbon nanotubes, while introducing a pseudocapacitive charge storage mechanism through judicious functionalization. The effect on the capacitance of functionalizing with conjugated polymers, conducting polymers, and ruthenium oxide, are reported here. Through functionalization at the nanoscale level, improvements to capacitance were realized.

-----

14. **KEYWORDS, DESCRIPTORS or IDENTIFIERS** (Technically meaningful terms or short phrases that characterize a document and could be helpful in cataloguing the document. They should be selected so that no security classification is required. Identifiers, such as equipment model designation, trade name, military project code name, geographic location may also be included. If possible keywords should be selected from a published thesaurus, e.g., Thesaurus of Engineering and Scientific Terms (TEST) and that thesaurus identified. If it is not possible to select indexing terms which are Unclassified, the classification of each should be indicated as with the title.)

carbon nanotube, conducting polymer, ruthenium oxide, capacitance, supercapacitor